Am J Physiol Cell Physiol 320: C794–C805, 2021.
First published March 24, 2021; doi:10.1152/ajpcell.00420.2020

american physiological society

AMERICAN JOURNAL OF PHYSIOLOGY
CELL PHYSIOLOGY

RESEARCH ARTICLE

Making Cell Culture More Physiological

Porcine colonoids and enteroids keep the memory of their origin during regeneration

Alicia M. Barnett,[1,2] Jane A. Mullaney,[1,2,3] Charlotte Hendriks,[1,2] Lisa Le Borgne,[1,2] Warren C. McNabb,[2,3] and Nicole C. Roy[2,3,4]

[1]*AgResearch Ltd, Grasslands Research Centre, Palmerston North, New Zealand;* [2]*Riddet Institute, Massey University, Palmerston North, New Zealand;* [3]*The High-Value Nutrition National Science Challenge, Auckland, New Zealand; and* [4]*Department of Nutrition, The University of Otago, Dunedin, New Zealand*

Abstract

The development of alternative in vitro culture methods has increased in the last decade as three-dimensional organoids of various tissues, including those of the small and large intestines. Due to their multicellular composition, organoids offer advantages over traditionally used immortalized or primary cell lines. However, organoids must be accurate models of their tissues of origin. This study compared gene expression profiles with respect to markers of specific cell types (stem cells, enterocytes, goblet, and enteroendocrine cells) and barrier maturation (tight junctions) of colonoid and enteroid cultures with their tissues of origin and colonoids with enteroids. Colonoids derived from three healthy pigs formed multilobed structures with a monolayer of cells similar to the crypt structures in colonic tissue. Colonoid and enteroid gene expression signatures were more similar to those found for the tissues of their origin than to each other. However, relative to their derived tissues, organoids had increased gene expression levels of stem cell markers *Sox9* and *Lgr5* encoding sex-determining region Y-box 9 and leucine-rich repeat-containing G protein-coupled rector 5, respectively. In contrast, expression levels of *Occl* and *Zo1* encoding occludin and zonula occludens 1, respectively, were decreased. Expression levels of the cell lineage markers *Atoh1*, *Cga*, and *Muc2* encoding atonal homolog 1, chromogranin A, and mucin 2, respectively, were decreased in colonoids, whereas *Sglt1* and *Apn* encoding sodium-glucose transporter 1 and aminopeptidase A, respectively, were decreased in enteroids. These results indicate colonoid and enteroid cultures were predominantly comprised of undifferentiated cell types with decreased barrier maturation relative to their tissues of origin.

barrier maturation; colon; differentiation; intestinal epithelium; stem cells

BACKGROUND

There are differences in the structure and function of the two distinct anatomical sections of the intestinal tract, the small and large intestine (1). The most obvious difference is the presence of the crypt-villi domains in the small intestine that begin within the crypts of Leiberkühn deep within the submucosa and extend as multiple finger-like villus projections toward the lumen. Although the large intestine has crypt domains that also extend into the submucosa, villi are absent (1). The small intestinal villi increase the surface area, thus functionally increasing the absorption of readily available nutrients. The large intestine completes the absorption process, and its primary function is to retrieve water and sodium from the luminal contents, which become fecal residue (1).

A more subtle difference between the small and large intestines relates to the cellular composition of the epithelium in these regions. The epithelium is a continuous monolayer of cells that is replenished from the nondifferentiated stem and progenitor cells located in the crypt domains (2). Differentiated Paneth cells are only found at the base of the crypts of the small intestine (1). Other differentiated cell types are predominantly found in the villi of the small intestine and the upper crypt region and surface epithelium of the colon (3, 4). Enterocytes are the most representative cell type of the small intestine, whereas the abundance of goblet cells increases from the duodenum (4%) to the distal colon (16%–24%) (5–9). Enteroendocrine cells are present in both segments but represent less than 1% of epithelial cells (1). Together, these epithelial cells form the intrinsic barrier, of which junctional proteins such as occludin, claudin, and zonula occludens are important components (10) that regulate barrier function, controlling the entry of luminal nutrients, ions, and water (11).

Correspondence: A. M. Barnett (alicia.barnett@agresearch.co.nz).
Submitted 26 August 2020 / Revised 16 March 2021 / Accepted 16 March 2021

Although the differences in structure, function, and cellular composition in the small and large intestines occur in vivo, it has been challenging to translate these differences to long-term in vitro culture models. With the advent of organoid technology, creating cultures with multiple cell types has become increasingly popular. To date, intestinal organoid cultures have been developed for many species including human, mouse, and pig (3, 12–15). Organoids generated from various regions of the intestinal tract are given descriptors according to their original site of isolation. For example, organoid units from the stomach are termed gastroids, whereas enteroids represent those derived from the small intestine (duodenum, jejunum, and ileum) and colonoids are those from the large intestine. Regardless of the site of origin, intestinal stem cells that reside in the tissue microenvironment or compartment known as the stem cell niche can be isolated and cultured in vitro into self-organizing, multicellular structures (16). Only stem cells have regenerative capabilities; thus, maintaining the stem cell niche in vitro is essential for the longevity of organoids over multiple passages in culture.

Although it is possible to isolate and culture stem cells from the intestine, most published studies relate to enteroid cultures derived from the small intestine such as duodenum (17), jejunum (13, 18–20), or ileum (15). Colonoid cultures have been developed from mouse and human, but it is often difficult to obtain human tissue (21). The porcine intestine is a suitable alternative to human intestine because it has greater morphological and functional similarities than that of the mouse and has previously been used by researchers as a model to study intestinal development, disease, and nutrition (22).

In this study, we hypothesized that colonoids and enteroids would be similar in cellular composition and differentiation to the tissues they originate from and are therefore suitable models of the intestinal epithelium. We used published methods for the isolation and culture of porcine enteroids and applied them with minor modifications to the isolation and culture of porcine colonoids. Organoid cultures and the tissues from which they were derived were characterized by determining the mRNA expression of known markers of specific cell types (stem cells, enterocytes, and goblet and enteroendocrine cells) and barrier maturation (tight junctions). Expression levels were compared between *1*) an epithelial fraction from ileum and colon tissue; *2*) enteroid and colonoid cultures and their respective tissues of origin; and *3*) colonoid and enteroid cultures.

MATERIALS AND METHODS

Buffers and Media

The buffers and media are as follows:

Wash buffer: ice-cold phosphate-buffered saline (PBS; Thermo Fisher, Auckland, New Zealand).

Dissociation buffer: PBS, 2 mM ethylene diamine tetra acetic acid (EDTA; Sigma-Aldrich, Auckland, New Zealand).

Basal medium 1 (BM1): advanced DMEM/F12 (ADF) supplemented with GlutaMAX (2 mM, Gibco, Life Technologies, Auckland, New Zealand) and HEPES (10 mM, Life Technologies).

Conditioned media: The method for the generation of conditioned media (CM) from L-WRN cells (American Type Culture Collection (ATCC), Manassas, VA, CRL-3276) producing the growth factors Wnt-3A, R-spondin 3, and noggin has been described in detail by (23).

Complete conditioned medium (CCM): BM1 was combined with CM at a 1:1 ratio. The following chemicals were purchased from Sigma-Aldrich, Auckland, New Zealand, and added gastrin (15 nM), nicotinamide (10 mM), N-acetyl-cysteine (1.25 mM), human recombinant epidermal growth factor (hEGF—50 ng/mL), p38 mitogen-activated protein kinase (MAPK) inhibitor (SB202190—10 μM), and transforming growth factor beta (TGFβ)-type receptor inhibitor (A83-01—600 nM). The RHO/Rho-associated coiled-coil kinase (ROCK) inhibitor (Y-27632—10 μM) was included in the culture medium during the initial 24 h of culture after isolation and after passaging only.

Freezing medium: 90% fetal bovine serum (FBS; In Vitro Technologies, Auckland, New Zealand) and 10% dimethyl sulfoxide (DMSO; Sigma-Aldrich), which made fresh on the day of freezing.

Animals and Sample Collection

Tissues were obtained from three healthy male pigs (PIC Camborough 46 × PIC boar 356 L) 12 wk of age euthanized for reasons unrelated to this project. The ethics approval was obtained from the Animal Ethics Committee, Massey University, Palmerston North, New Zealand. Animals were anaesthetized with an intramuscular injection of an anesthetic cocktail [0.04 mL/kg body weight (BW) of Zoletil 100 (50 mg/mL), ketamine (50 mg/mL), and xylazine (50 mg/mL); Provet]. Immediately after sedation, the pigs were euthanized by an intracardial injection of sodium pentobarbitone (0.3 mL/kg BW of Pentobarb 300; Provet).

Isolation of Crypts from Pig Intestine and Culture of Organoids

The method to generate porcine organoids has been described in part elsewhere (12, 15, 24) and was used with minor modifications. Briefly, sections ~8–10 cm in length were collected from the proximal ileum and proximal colon of three male pigs. After washing in cold PBS, the outer muscle layer was removed from the tissue, and sections opened longitudinally. Once opened, sections were washed thoroughly using ice-cold PBS to remove digesta and the mucus layer. For ileal sections, the epithelial surface of the tissue was scraped using a glass microscope slide to remove the villi. The tissue was cut into pieces approximately 5 mm^2 and washed repeatedly using a vortex (maximum speed for 10 s) until the buffer was clear (~5–10 washes). After the final wash, the tissue was incubated with dissociation buffer for 30 min on ice on a rocking platform and then rinsed gently with ice-cold PBS to dislodge any remaining villous components from the tissue. For crypt collection, the tissue pieces were transferred to a 100-mm Petri dish (In Vitro Technologies). A glass slide was placed over the tissue, and pressure was applied to force the crypts to separate from the tissue. The number of crypts released was observed using a light microscope (Eclipse TS100 inverted microscope, Nikon, Japan). The collected crypts were centrifuged at 200 *g* for

5 min at 4°C (Eppendorf 5804 R centrifuge, using rotor S-4–72) and suspended in ice-cold BM1. The number of crypts in the suspension was determined, and the volume required for seeding was calculated. Typically, 300 crypts per well were used as an initial seeding density, because seeding at densities less than or greater than 300 crypts can inhibit colonoid development. The required volume of crypt suspension was centrifuged at 200 *g* for 3 min at 4°C, and the crypts were gently suspended in ice-cold CCM. Cold, liquid Cultrex (Cultrex PathClear reduced growth factor basement membrane matrix; R&D Systems, In Vitro Technologies Ltd.) was combined gently with the suspended crypts (at a 1:1 ratio), and 30 μL of the crypt and matrix mix was added to each well of a 24-well plate. The plate was inverted and placed in the incubator to allow the matrix to polymerize. This step ensures that the crypts were suspended in the matrix as opposed to settling and sticking to the surface of the plate. After 15 to 30 min, 500 μL of CCM containing the RHO/ROCK inhibitor (10 μM) was added to each well, and the cultures incubated at 37°C in a 5% CO_2-humidified atmosphere. The medium was changed in each well after the first 24 h and replenished with CCM without RHO/ROCK inhibitor, with additional medium changes every 48 h.

The available crypt fraction from each tissue, which was surplus to seeding requirements, was collected for downstream RNA extraction and used to represent the colon and ileum tissue samples in the qPCR analysis. These fractions were lysed with 1 mL TRI Reagent (Life Technologies, Auckland, New Zealand), and samples were stored at −80°C until RNA isolation.

Plating Efficiency

Plating efficiency was determined by calculating the number of organoids growing on *day* 7 as a percentage of the total number of crypts that had been plated. The plating efficiency for organoid establishment was tracked for each colonoid culture from three animals. In total, six wells were plated with colon crypts from each animal. Plating efficiency % = (number of crypts growing after 7 days/by the number of crypts seeded) × 100%.

Passaging of Organoids

Enteroids and colonoids were passaged at a 1:5 ratio every 5 to 7 days through mechanical disruption and reseeded into 24-well plates in fresh Cultrex droplets. Briefly, media was removed, and 500 μL of ice-cold PBS was added to each well to depolymerize the Cultrex matrix. The organoid structures were mechanically disrupted by repeatedly passing through a syringe with a 25-gauge needle attached and centrifuged at 100 × *g* for 4 min at 4°C. The Cultrex and PBS solutions were removed, and the disrupted organoid units resuspended in ice-cold CCM and Cultrex combination and seeded into 24-well plates as described above.

Cryopreservation of Organoids

Enteroids and colonoids were cryopreserved at different passages. Briefly, cultures were allowed to reform enteroid and colonoid structures for 3-5 days postpassaging. The media was removed from each well, and the matrix depolymerized using 500 μL of ice-cold PBS. Samples were centrifuged at 100 *g* for 4 min at 4°C. The PBS and Cultrex solutions were removed and replenished with 1 mL freezing media. Organoid units from two wells cultured from the same animal and at the same passage number were combined and frozen down into a single vial (Corning, Lindfield, Sydney, Australia). Vials were stored overnight at −80°C in a Nalge Nunc Cryo 1°C Mr Frosty Freezing Container (Thermo Fisher Scientific, Auckland, NZ) and then transferred into a liquid nitrogen cell dewar for long-term storage.

Culture of Organoids

Newly passaged organoid units from ileum and colon were cultured for 24 h in CCM containing the RHO/ROCK inhibitor (10 μM) and then transferred to CCM without RHO/ROCK inhibitor with medium changes every 48 h. Enteroids and colonoids were cultured for an additional 120 h in CCM after which point the media was removed, and 500 μL of ice-cold PBS was added to each well to depolymerize the Cultrex matrix. Samples were centrifuged at 100 *g* for 4 min at 4°C, and the Cultrex and PBS solutions were removed. Cultures were lysed using 500 μL of TRI Reagent (Life Technologies), and samples were stored at −80°C until RNA isolation.

Histological and Immunofluorescence Analyses

Ileum and colon tissue samples were washed with ice-cold PBS, fixed in 10% neutral buffered formalin, and embedded in paraffin. Tissue sections (5–8 μm thickness; Massey University Histology Facility, Palmerston North, NZ) were stained with hematoxylin and eosin (H&E).

Immunofluorescent staining of tissue sections was carried out using standard protocols for paraffin removal and antigen retrieval with 10 mM citrate buffer. Briefly, sections on slides were placed in xylene and ethanol for de-paraffinization and rehydration. Sections were incubated in a water bath at 95°C for 30 min and cooled on the benchtop for 30 min to unmask the antigen, followed by gentle rinsing with water for 5 min. Sections were incubated with primary antibody to sex-determining region Y (SRY)-box 9 (*Sox9*) conjugated to Alexa Fluor488; Abcam ab196450; research resource identifier (RRID) AB_2665383; 1:200 (25), zonula occludens 1 (Zo1), Thermo Fisher Scientific 339100; RRID:AB_87181; 1:500 (15) or mucin 2 (Muc2), Santa Cruz; sc-515032; RRID: AB_2815005; and 1:100 (26) at room temperature for 60 min. After rinsing three times with PBS, sections were incubated with appropriate secondary antibody either Alexa Fluor488/Goat Anti-Mouse IgG; Abcam ab150113, RRID:AB_2576208; and 1:1,000 (26) in the dark for further 60 min. Sections were again rinsed three times with PBS and stained with DAPI (Thermo Fisher Scientific, D1306, RRID:AB_2629482—1:1,000). Sections were mounted using ProLong Gold Antifade (Life Technologies, P36934, RRID:SCR_015961), and coverslips sealed with clear nail varnish.

Colonoids were seeded and cultured for 7 days on 13-mm round coverslips. Media was removed, and domes washed twice with warm PBS. Colonoids were fixed with 4% paraformaldehyde and PBS solution at room temperature for 20 min, washed again with warm PBS and permeabilized with 0.2% Triton X-100 (Sigma-Aldrich) in PBS for 30 min at room temperature. Cultures were washed with warm PBS and incubated with phalloidin conjugated to Alexa Fluor546

(Life Technologies, A22283, RRID:AB_2632953) in the dark for 60 min at room temperature or primary antibody to *Sox9* conjugated to AlexaFluor647; Abcam ab196184, RRID: AB_2813853; and 1:200 (27) or Muc2 (1:100) at room temperature for 60 min. After rinsing three times with PBS, colonoids were incubated with secondary antibody Alexa Fluor488/ Goat Anti-Mouse IgG (1:1,000) in the dark for further 60 min. Colonoids were washed with warm PBS and stained with DAPI (1:1,000) before coverslips were transferred and mounted on glass slides.

Tissue sections and colonoids were visualized on a Nikon Eclipse Ti-S inverted fluorescence microscope (Nikon, Tokyo, Japan) fitted with a digital Nikon DS-Ri2 camera (Nikon, Tokyo, Japan). Images were captured using NIS-Elements software (v4.40).

Quantitative Real-Time PCR

Total RNA was isolated using the Direct-zol RNA purification kit (Zymo Research, Irvine, CA) and treated with DNase I during RNA isolation to remove genomic DNA. RNA quantity and quality for all samples were determined by optical density (OD 260/280) measurements using a NanoDrop 1000 Spectrophotometer (Thermo Fisher Scientific, Auckland, New Zealand). Before downstream analysis, an Agilent 2100 Bioanalyzer (Agilent Technologies, Santa Clara, CA) was used to ensure all samples had an RNA integrity number (RIN) above 8.0. RNA (275 ng) was reverse-transcribed using an RNA High Capacity RNA-to-cDNA kit (Applied Biosystems 4387406, Foster City, CA). For the qPCR, the PowerUp SYBR Green Master Mix Lo-ROX Kit (Applied Biosystems, A25780) was used on a QuantStudio3 Real-Time PCR System (Applied Biosystems) in a MicroAmp Fast Optical 96-Well Reaction Plate (0.1 mL) covered with MicroAmp Clear Adhesive Film (Applied Biosystems). For the qPCR, 1 μL of cDNA (diluted 3:4 with nuclease-free water; Life Technologies) was used as a template (excluding the no template controls where 1 μL of nuclease-free water was used) in a 10 μL reaction where the following conditions were applied: 2 min at 50°C, 10 min at 95°C followed by 40 cycles of two-step PCR denaturation at 95°C for 15 s, and annealing extension at 60°C for 60 s.

The primers used were designed based on published sequences and using the NCBI online primer design tool (Primer-BLAST, http://www.ncbi.nlm.nih.gov/tools/primer-blast/). The primers were designed to detect target gene expression of known markers of specific cell types and barrier maturation. Leucine-rich repeat-containing G protein-coupled receptor 5 (*Lgr5*), olfactomedin 4 (*Olfm4*), and sex-determining region Y (SRY)-box 9 (*Sox9*) were selected as known targets for stem cells, and for differentiated cell types including enterocytes, goblet cells, and enteroendocrine cells, known primers for sodium-glucose transporter 1 (*Sglt1*), mucin 2 (*Muc2*), and chromogranin A (*Cga*), respectively, were used. Because the colon has an increased abundance of secretory cells relative to the small intestine (6, 7, 9), we used atonal homolog 1 (*Atoh1*) as a known indicator of secretory cell fate. Maturation and differentiation of enterocytes and colonocytes were investigated with primers to aminopeptidase N (*Apn*) and carbonic anhydrase 2 (*Ca2*), respectively. Other properties of barrier maturation were examined using primers to the junctional proteins, occludin (*Occl*), *Zo1*, and claudin (*Cldn*). All primers were purchased from Integrated DNA Technologies (IDT, Coralville, IA). The genes of interest and the primers used in this study are given in Table 1.

The data were normalized to the geomean of the stably expressed reference genes *Tbp* and *Rpl4* and examined for expression-level changes using the comparative delta-delta cycle threshold (ΔΔCt) method (31). For example, in this method the fold change = $2^{\Delta\Delta Ct}$ where $\Delta\Delta Ct = [Ct_{(geomean)} - Ct_{(target\ gene)colonoid} - Ct_{(geomean)} - Ct_{(target\ gene)enteroid}]$. Data collected from the epithelial tissue fraction or organoid cultures from three pigs were compared to samples from the same pig and reported as average $\log_2$-fold change ± SD.

Statistical Analysis

Statistical analysis was undertaken using SigmaPlot version 14.0 and GraphPad Prism version 9. Normally distributed data as determined from the Shapiro–Wilk test were analyzed by a two-tailed Student's *t* test with Welch's

Table 1. *List of primers used for qPCR*

Gene	Primer Sequences (5′ to 3′)		Reference
	Forward	Reverse	
Tbp	aac agt tca gta gtt atg agc cag a	aga tgt tct caa acg ctt cg	(28)
Rpl4	caa gag taa cta caa cct tc	gaa ctc tac gat gaa tct tc	(28)
Lgr5	cct tgg ccc tga aca aaa ta	att tct ttc cca ggg agt gg	(12)
Olfm4	gtc agc aaa ccg gct att gt	tgc ctt ggc cat agg aaa ta	(12)
Sox9	cgg ttc gag caa gaa taa gc	gta atc cgg gtg gtc ctt ct	(12)
Atoh1	cac ggg ctg aac cac gcc tt	ggt acc cgc gct tgc ttc gt	(12)
Sglt1	gca gct gtc ttc cta ctt gc	gca aac tcg gta atc ata cgg	(12)
Cga	gac cag act gag ttg aag	gcg tct tca tcg ttc tt	This study
Muc2	cat cca ctc caa cat ctc	cgg gac aca ctt ctt ac	This study
Apn	caa tat gcc gcc caa agg ttc	ccg gat cag gac gcc att t	(29)
Ca2	ctc ttg ctg gca ctt ac	gta gct ctg cag cat att	This study
Ocln	tcc tgg gtg tga tgg tgt tc	cgt aga gtc cag tca ccg ca	(30)
Zo1	aag ccc taa gtt caa tca caa tct	atc aaa ctc agg agg cgg c	(30)
Cldn1	aga aga tgc gga tgg ctg tc	ccc aga agg cag aga gaa gc	(30)

Apn, aminopeptidase N; *Atoh*, atonal homolog 1; *Ca2*, carbonic anhydrase 2; *Cga*, chromogranin A; *Cldn*, claudin; *Lgr5*, leucine-rich repeat-containing G protein-coupled receptor; *Muc2*, mucin 2; *Olfm4*, olfactomedin 4; *Sox9*, sex-determining region Y-box 9; *Sglt1*, sodium-glucose transporter 1; *Tbp*, tata box protein; *Zo1*, zonula occludens 1.

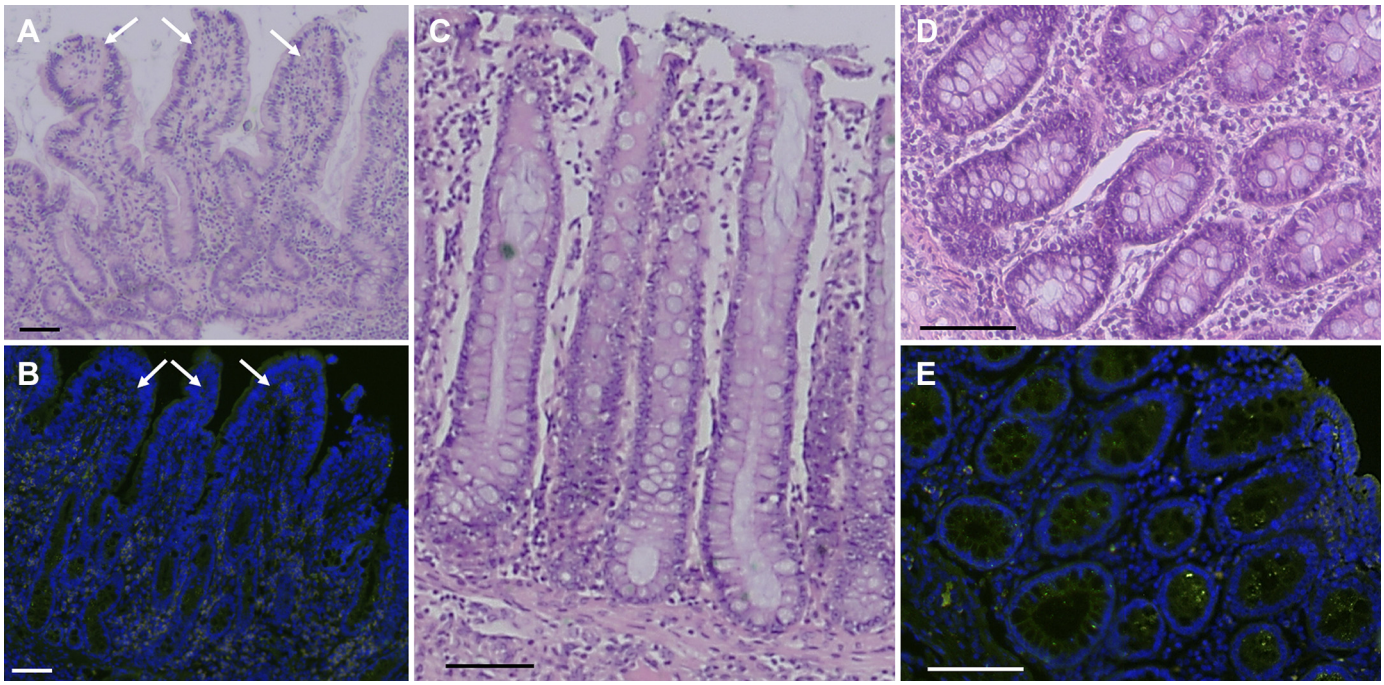

Figure 1. Histological and immunofluorescence staining of porcine ileum (*A–B*) and colon (*C–E*) tissue. Sections stained with hematoxylin and eosin (H&E) indicate the presence of villus compartments (white arrows) in ileum tissue (*A*) that are absent in colon tissue (*C*) which instead have deep, pit-like crypts that extend from bottom to top. Immunofluorescence staining of zonula occludens (Zo1—green) and nuclei (blue) indicates that villi (white arrows) and crypts of the ileum (*B*) are comprised of a single layer of cells. A single layer of cells is also evident in a cross section of porcine colon crypts stained with H&E (*D*) and immunofluorescent staining of Zo1 protein and nuclei (*E*). Scale bar represents 100 μm. Zo1, zonula occludens.

correction, or if the data did not fit a normal distribution, the Mann–Whitney *U* test was used. Data are presented as means ± SD, and significance was taken as $P < 0.05$ with a confidence interval of 95%. qPCR data were analyzed with principal component analysis (PCA) using the mixOmics package (32) in R version 4.0.0 where an unsupervised linear transformation was applied to the data set (delta Ct values) to reduce dimensionality and find the key features that discriminate the groups.

RESULTS

Colonoids Share Structural Similarity with Colonic Tissue

First, crypts were isolated from ileum and colon tissues and visualized. Histological examination of fixed porcine ileal and colonic tissues was used to highlight structural differences between them (Fig. 1). As expected, the villus structures were evident in ileum sections as multiple projections extruding upward from the basally located crypts (Fig. 1, *A–B*). These extrusions were absent in colon sections (Fig. 1*C*), which instead have a pit-like structure from bottom to top. Both the villi and crypts of the ileum (Fig. 1*B*) and crypts of the colon (Fig. 1, *D–E*) were formed from a continuous monolayer of cells.

Before isolation of the crypts from ileum tissue, the villus compartments were removed from the epithelial surface through scraping, to reduce the harvesting of undesirable differentiated cell types that would hamper the development of enteroids. As a result of this, the crypts isolated from the ileum were not as elongated and contained fewer cells relative to those isolated from the colon tissue (Fig. 2, *A* and *B*, respectively).

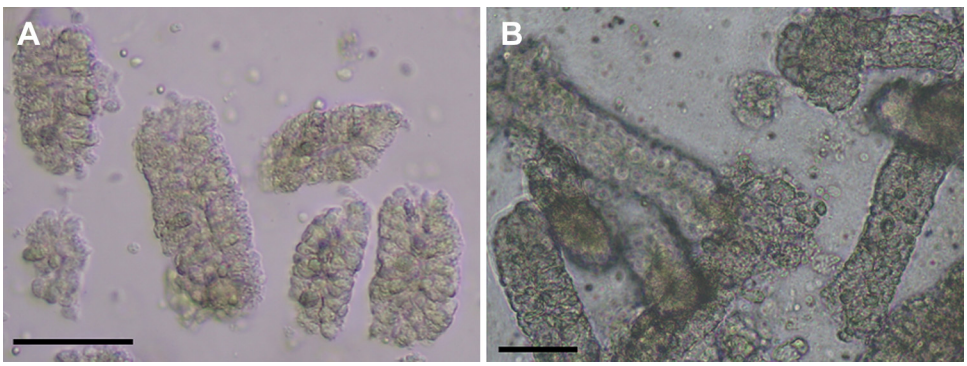

Figure 2. Bright-field images of isolated crypts from porcine ileum (*A*) and colon (*B*) tissue. Scale bar represents 100 μm.

Twenty-four hours postisolation, colon crypts formed simple spheroids. These structures had a single layer of epithelial cells around a central lumen-like structure (Fig. 3*A*) similar to that evidenced in the cross section from fixed colon tissue (Fig. 1, *D–E*). Spheroids formed budding structures after 3–5 days in culture (Fig. 3*B*), and from *day* 7, multilobed colonoid structures were evident (Fig. 3, *C–D*). There was a significant increase in the plating efficiency of colonoids that were isolated from pig 1 (83% ± 8.0) as compared to both pig 2 (63% ± 4.5) and pig 3 (70% ± 4.1) that were more similar to each other (Fig. 3*E*). Immunofluorescent staining was used to show that specific cell types were present in both the native colon tissue and colonoids after 7 days of culture. *Sox9*, a recognized marker for stem cells, was detected in cells at the base of the colonic crypts (Fig. 3*F*) and present in colonoid structures (Fig. 3*H*). Staining for Muc2 marked mucus-producing goblet cells in colon tissue (Fig. 3*G*) and in discrete locations in colonoids (Fig. 3*I*).

Gene Expression Profiling

The mRNA expression levels of markers for specific cell types, differentiation, and barrier maturation were determined for organoid cultures and the tissue from which they were derived.

First, we compared colon and ileum tissue to determine what effect tissue specificity had on gene expression profiles. In colon tissue, mRNA expression levels of the stem cell markers *Olfm4* and *Sox9* were 4.1-fold lower and 5.9-fold higher, respectively, relative to the ileum (Fig. 4). As expected, the mRNA expression levels of absorptive enterocyte or colonocyte marker *Sglt1* and enterocyte differentiation marker *Apn* were significantly lower (0.02-fold ± 0.01-fold and 0.03-fold ± 0.02-fold, respectively). The mRNA abundance of the secretory goblet cell marker *Muc2* and colonocyte differentiation marker *Ca2* was significantly higher (1.6-fold ± 0.5-fold and 10.9-fold ± 2.3-fold, respectively) in

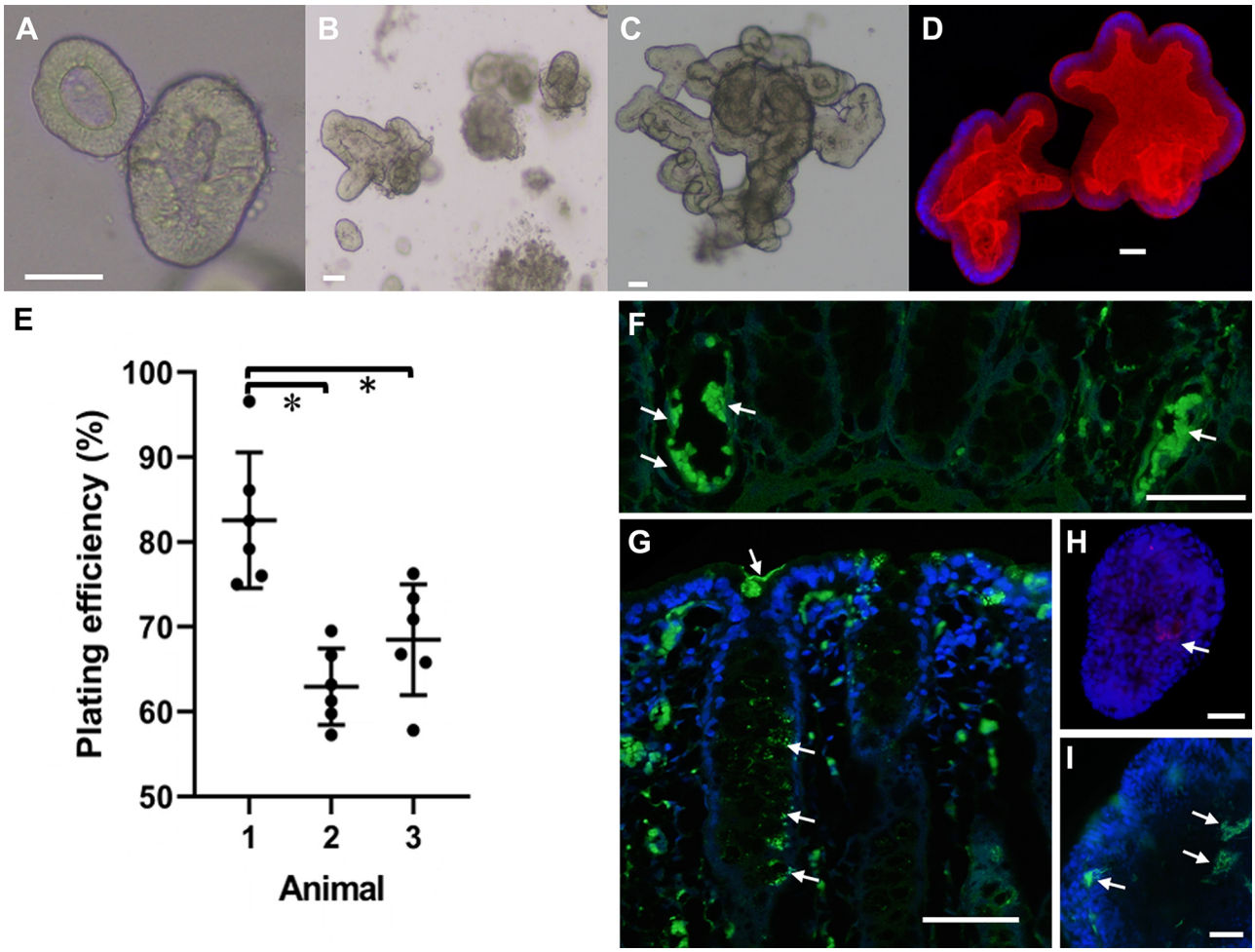

Figure 3. Temporal development of porcine colonoids. Twenty-four hours postisolation of porcine colon crypts, spheroid structures are formed (*A*). After 3 days, spheroids form budding structures (*B*), and from 7 days of continuous culture, multilobed structures are formed (*C* and *D*). Immunofluorescent staining of F-actin (red) and nuclei (blue) indicates that colonoids have a monolayer of cells around a central lumen-like void as evidenced by the stained nuclei at the perimeter of the structure (*D*). Plating efficiency of colonoid development was determined for each colonoid culture from three individual animals (*E*). In total, six wells from each animal were plated with crypts and the number of colonoids established after 7 days of culture was determined. Data are presented as scatter dot plots, where the mean and SD are shown (*E*). Data were analyzed using two-tailed Student's *t* test with Welch's correction, and values considered to have statistical significance ($P < 0.05$) are denoted by *. Immunofluorescent staining for specific cell types in colon tissue (*F* and *G*) and in colonoids (*H* and *I*) after 7 days of culture. Antibodies for *Sox9*, stem cells (*F* and *H*), and Muc2 for goblet cells (*G* and *I*) detected the same cell types in both colon tissue and colonoids as indicated by white arrows (*F–I*). Scale bar represents 100 μm. Sox9, sex-determining region Y (SRY)-box 9.

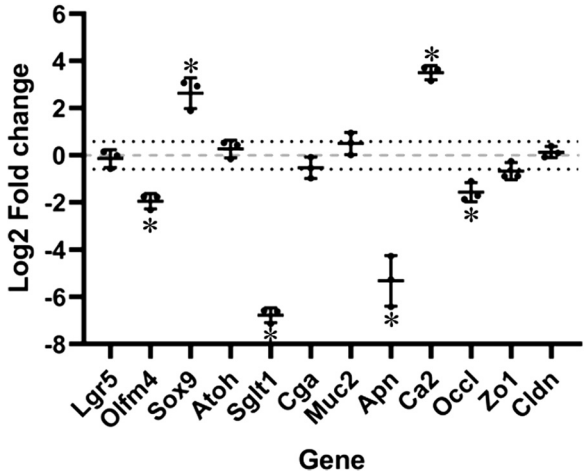

Figure 4. Differential gene expression between colon tissues relative to ileum as determined by qPCR. The relative quantitative expression of stem cell markers (*Lgr5*, *Olfm4*, and *Sox9*), secretory cell fate (*Atoh*), specific, differentiated cell types (*Sglt1*—a marker for absorptive enterocytes/colonocytes, *Cga*—enteroendocrine cell, and *Muc2*—goblet cell), and differentiation (*Apn* and *Ca2*) and markers of barrier maturation (*Occl*, *Zo1*, and *Cldn*) mRNA transcripts from colon tissue relative to the ileum (n = 3 individual animals). Extracted RNA was used for real-time quantitative reverse transcription-polymerase chain reaction (qRT-PCR). Data are presented as the $\log_2$-fold changes in transcript levels normalized to expression of the ileum fraction and shown as scatter dot plots; mean is shown, and whiskers represent SD. Data were analyzed using two-tailed Student's t test with Welch's correction. Values below −0.585 and above 0.585 (corresponding to 1.5-fold change) are indicated by the dashed lines and were considered to have statistical significance ($P < 0.05$) denoted by *. *Apn*, aminopeptidase N; *Atoh*, atonal homolog 1; *Ca2*, carbonic anhydrase 2; *Cga*, chromogranin A; *Cldn*, claudin; *Lgr5*, leucine-rich repeat-containing G protein-coupled receptor; *Muc2*, mucin 2; *Olfm4*, olfactomedin 4; *Sox9*, sex-determining region Y-box 9; *Sglt1*, sodium-glucose transporter 1; *Zo1*, zonula occludens 1.

colon relative to the ileum. mRNA expression levels of *Occl* were significantly lower (0.38-fold ± 0.1-fold) in colon relative to the ileum (Fig. 4).

We next compared organoid cultures to their parental tissues and then to each other. Stem cell mRNA expression is elevated in enteroids relative to the ileal tissue *Olfm4*. mRNA expression levels were significantly elevated (2.1-fold ± 0.8-fold) in enteroid cultures relative to ileal tissue (Fig. 5), whereas the mRNA abundance of *Sox9* was significantly increased (9.1-fold ± 1.7-fold). Levels of *Atoh1*, *Cga*, and *Muc2* mRNA were unchanged ($P > 0.05$), but in contrast, *Sglt1* and *Apn* mRNAs were both significantly lower (0.04-fold ± 0.01-fold and 0.02-fold ± 0.01-fold, respectively). *Occl* and *Zo1* mRNA expression levels were not significantly different, but *Cldn* was significantly elevated 8.6-fold ± 0.58-fold in enteroids relative to the ileum (Fig. 5).

Stem Cell mRNA Expression Is Elevated in Colonoids, While Secretory Cell Lineage Markers Are Decreased in Colonoids Relative to Colon Tissue

Colonoids had significantly elevated mRNA expression levels of *Lgr5* and *Sox9* (9.3-fold ± 1.8-fold and 5.2-fold ± 0.2-fold, respectively) relative to the colon, whereas *Olfm4* was significantly lower at 0.2-fold ± 0.08-fold (Fig. 6). *Sglt* and *Ca2* mRNA levels were not different, but *Atoh1*, *Cga*, and *Muc2* were all significantly lower in colonoids versus tissue. In addition, mRNA expression levels of *Occl* and *Zo1* were also lower, whereas *Cldn* was significantly elevated (4.2-fold ± 0.9-fold) in colonoids relative to the colon (Fig. 6). These results indicate that the stem cell niche of colonoid cultures is being maintained but that secretory cell lineages are decreased relative to the tissue from which they were derived, resulting in predominantly immature, undifferentiated structures.

Colonoids Have mRNA Expression Profiles Distinct from Enteroids

The mRNA expression profiles of selected targets were significantly different in colonoids relative to enteroid cultures (Fig. 7). mRNA expression levels of *Lgr5* and *Sox9* were significantly elevated by 4.5-fold ± 1.1-fold and 3.2-fold ± 0.5-fold, respectively, whereas *Olfm4* was significantly reduced (0.03-fold ± 0.01-fold). mRNA expression levels of *Atoh1*, *Cga*, and *Muc2* were also all significantly lower in colonoids relative to enteroids. As expected, colonoids had significantly elevated mRNA levels of *Ca2* (25.8-fold ± 3.2-fold) and significantly lower *Sglt1* (0.2-fold ± 0.06-fold) and *Apn* (0.3-fold ± 0.01-fold). In addition, *Occl Zo1* and *Cldn* mRNA expression levels were also lower (0.2-fold ± 0.01-fold, 0.3-fold ± 0.06-fold, and 0.5-fold ± 0.15-fold, respectively) in colonoids relative to enteroids (Fig. 7).

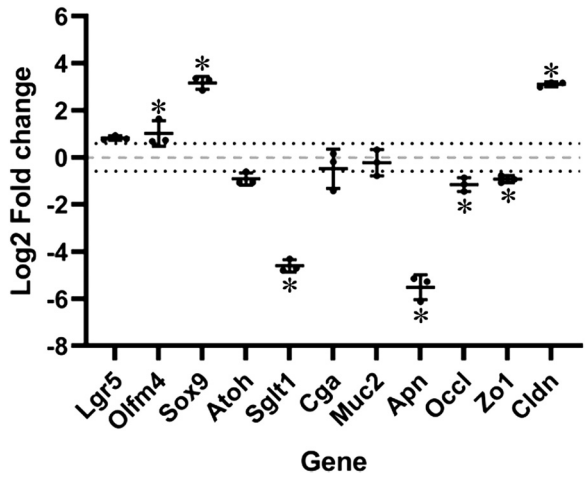

Figure 5. Differential gene expression between enteroid cultures relative to ileum as determined by qPCR. The relative expression of markers of stem cell (*Lgr5*, *Olfm4*, and *Sox9*), secretory cell fate (*Atoh*), specific, differentiated cell types (*Sglt1*—a marker for absorptive enterocytes/colonocytes, *Cga*—enteroendocrine cell, and *Muc2*—goblet cell), and differentiation (*Apn* and *Ca2*) and markers of barrier maturation (*Occl*, *Zo1*, and *Cldn*) mRNA transcripts in enteroid cultures relative to an epithelial fraction from ileum tissue (n = 3 individual animals) as determined from qPCR. Data are presented as $\log_2$-fold change normalized to ileum fraction and shown as scatter dot plots; mean is shown, and whiskers represent SD. Data were analyzed using Mann–Whitney U test. Values below −0.585 and above 0.585 (corresponding to 1.5-fold change) are indicated by the dashed lines and were considered to have statistical significance ($P < 0.05$) denoted by *. *Apn*, aminopeptidase N; *Atoh*, atonal homolog 1; *Ca2*, carbonic anhydrase 2; *Cga*, chromogranin A; *Cldn*, claudin; *Lgr5*, leucine-rich repeat-containing G protein-coupled receptor; *Muc2*, mucin 2; *Olfm4*, olfactomedin 4; *Sox9*, sex-determining region Y-box 9; *Sglt1*, sodium-glucose transporter 1; *Zo1*, zonula occludens 1.

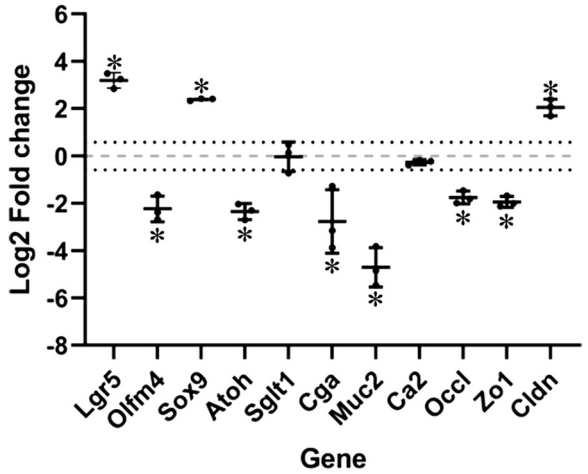

Figure 6. Differential gene expression between porcine colonoid cultures relative to the colon as determined by qPCR. The relative expression of markers of stem cell (*Lgr5*, *Olfm4*, and *Sox9*), secretory cell fate (*Atoh*), specific, differentiated cell types, (*Sglt1*—a marker for absorptive enterocytes/colonocytes, *Cga*—enteroendocrine cell, and *Muc2*—goblet cell), and differentiation (*Apn* and *Ca2*) and markers of barrier maturation (*Occl*, *Zo1*, and *Cldn*) mRNA transcripts in colonoid cultures relative to an epithelial fraction from colon tissue (n = 3 individual animals) as determined from qPCR. Data are presented as $\log_2$-fold change and shown as scatter dot plots; mean is shown, and whiskers represent SD. Data were analyzed using two-tailed Student's t test with Welch's correction. Values below −0.585 and above 0.585 (corresponding to 1.5-fold change) are indicated by the dashed lines and were considered to have statistical significance ($P < 0.05$) denoted by *. *Apn*, aminopeptidase N; *Atoh*, atonal homolog 1; *Ca2*, carbonic anhydrase 2; *Cga*, chromogranin A; *Cldn*, claudin; *Lgr5*, leucine-rich repeat-containing G protein-coupled receptor; *Muc2*, mucin 2; *Olfm4*, olfactomedin 4; *Sox9*, sex-determining region Y-box 9; *Sglt1*, sodium-glucose transporter 1; *Zo1*, zonula occludens 1.

Colonoids Maintain Their mRNA Profile over Time

The expression of selected cell markers was also assessed in low- (P2), medium- (P5), and high-passage (≥P10) colonoid cultures to determine whether mRNA levels changed as a consequence of passaging. Levels of mRNA were not significantly ($P > 0.05$) different for markers of stem cells (Fig. 8*A*), differentiated cell types (Fig. 8*B*), or barrier markers (Fig. 8*C*). This result indicates that passaging does not change the mRNA profile of colonoid cultures.

Colonoid and Enteroid Cultures Behave Most like Their Tissues of Origin

Principal component analysis (PCA) was applied to identify the features that discriminate the groups. The PCA biplot (Fig. 9) simultaneously plots samples and variables, in this case genes, as shown by arrows.

An analysis of the PC1 (horizontal x-axis) showed that it is heavily weighted by *Occl*, *Zo1*, *Atoh1*, and *Olfm4* and negatively by *Lgr5* and *Sox9*. *Atoh1* is highly correlated with *Zo1* (0.95), *Cga* (0.97), and *Occl* (0.97), whereas *Lgr5* is highly correlated with *Sox9* (0.79). Conversely, *Lgr5* is negatively correlated with *Atoh1* (0.98), *Muc2* (0.98), and *Zo1* (0.95). *Sox9* is also negatively correlated with *Apn* (0.96). PC2 is heavily weighted by *Cldn* and negatively by *Ca2*.

Sample types clustered discretely with no correlation between the ileum and colonoids (0.26, $P > 0.05$) or between enteroid and colonoid cultures (0.4, $P > 0.05$). The highest correlations were observed between the ileum and enteroids (0.77, $P < 0.01$) and colon and colonoids (0.58, $P < 0.05$), indicating that the organoid cultures' gene expression profiles were similar to the tissue they were derived from.

Colonoids had increased expression levels of *Sox9*, *Lgr5*, and *Cldn*, and colon tissue could be discriminated by gene expression levels of *Ca2*. Ileum tissue had increased expression of *Apn*, *Cga*, and *Occl*, but enteroids did not have any key genes to discriminate them.

DISCUSSION

Intestinal organoid cultures offer a unique advantage over traditional in vitro models because they more readily represent the cellular complexity and architecture of the intestinal epithelium. To date, colonoid cultures representative of the large intestine have been characterized for human and mouse, but not for porcine crypt stem cells. Here, we isolated these crypt cells from the colon of three healthy male pigs and established long-term porcine colonoid cultures utilizing similar methods and media composition published for porcine enteroid cultures (15, 17). The cultured colonoids closely mimicked the structure of the colon being formed from a continuous monolayer of cells as multilobed structures reminiscent of the crypt invaginations, with both stem and goblet cells present in the structures. In vitro models of the intestine are used to study the complex in vivo intestinal

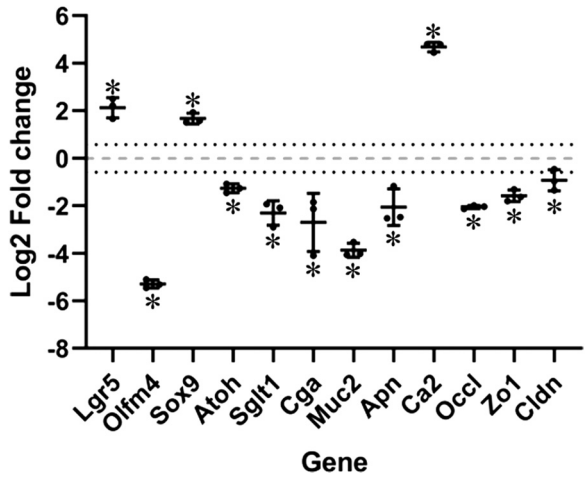

Figure 7. Differential gene expression between porcine colonoids relative to enteroid cultures as determined by qPCR. The relative expression of markers of stem cell (*Lgr5*, *Olfm4*, and *Sox9*) secretory cell fate (*Atoh*), specific, differentiated cell types, (*Sglt1*—a marker for absorptive enterocytes/colonocytes; *Cga*—enteroendocrine cell; and *Muc2*—goblet cell), and differentiation (*Apn* and *Ca2*) and markers of barrier maturation (*Occl*, *Zo1*, and *Cldn*) mRNA transcripts in colonoid cultures relative to enteroid cultures (n = 3 individual animals) as determined from qPCR. Data are presented as $\log_2$-fold change and shown as scatter dot plots; mean is shown, and whiskers represent SD. Data were analyzed using two-tailed Student's t test with Welch's correction. Values below −0.585 and above 0.585 (corresponding to 1.5-fold change) are indicated by the dashed lines and were considered to have statistical significance ($P < 0.05$) denoted by *. *Apn*, aminopeptidase N; *Atoh*, atonal homolog 1; *Ca2*, carbonic anhydrase 2; *Cga*, chromogranin A; *Cldn*, claudin; *Lgr5*, leucine-rich repeat-containing G protein-coupled receptor; *Muc2*, mucin 2; *Olfm4*, olfactomedin 4; *Sox9*, sex-determining region Y-box 9; *Sglt1*, sodium-glucose transporter 1; *Zo1*, zonula occludens 1.

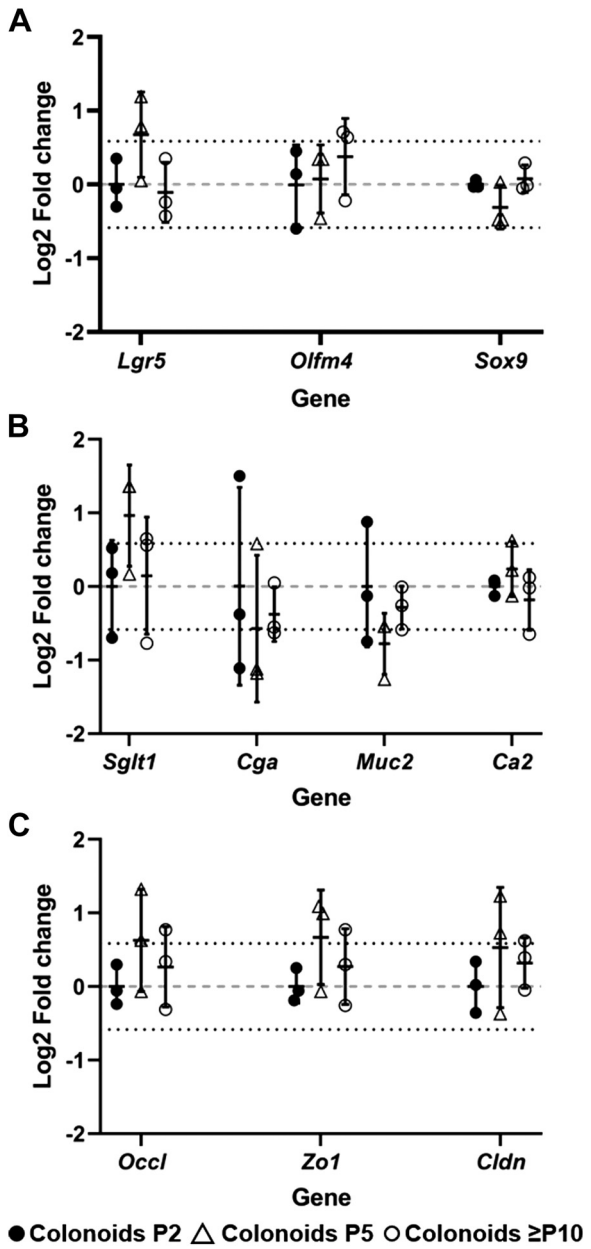

Figure 8. Gene expression of porcine colonoids at different passages as determined by qPCR. The relative expression of markers of stem cells (*A*), differentiated cell types and differentiation (*B*), and markers of barrier maturation (*C*) in colonoid cultures at passages (P) 2 (low passage—dark circles), P5 (medium passage—triangles), and ≥P10 (high passage—light circles). Data are presented as the $\log_2$-fold changes normalized to expression of P2 colonoids and shown as scatter dot plots where the mean is shown, and whiskers represent SD. Data were analyzed using two-tailed Student's *t* test with Welch's correction. Values are representative of triplicate colonoid cultures for each passage from three individual animals ($n = 3$). Values below −0.585 and above 0.585 (corresponding to 1.5-fold change) are indicated by the dashed lines and were considered to have statistical significance ($P < 0.05$). *Ca2*, carbonic anhydrase 2; *Cga*, chromogranin A; *Cldn*, claudin; *Lgr5*, leucine-rich repeat-containing G protein-coupled receptor; *Muc2*, mucin 2; *Olfm4*, olfactomedin 4; *Sox9*, sex-determining region Y-box 9; *Sglt1*, sodium-glucose transporter 1; *Zo1*, zonula occludens 1.

processes in a simplified context and allow for the evaluation of a cell's response under well-controlled and repeatable conditions (33). As such, these in vitro models need to be representative of their tissue of origin. Here, the enteroid and colonoid cultures derived from crypt stem cells were shown to maintain their genetic identity to their tissues of origin, and for colonoids levels, this could be maintained overall several passages. Indeed, colonoid cultures, as determined from the expression levels of genes encoding for markers of specific cell types (stem cells, enterocytes, goblet cells, and enteroendocrine cells) and barrier maturation (tight junctions), were most similar to an epithelial fraction from the colon. Similarly, the profile of enteroid cultures was most like the ileal tissue from which they were derived. It is thought that segment-specific expression is established and maintained as a result of intestinal stem cell-intrinsic DNA methylation patterns (34), and some genes such as *Lyz* (lysozyme), *Sglt1*, and *Cldn15* retain intestinal segment-specific expression with increased expression in ileum relative to colon (34). At the same time, *Ca2* is expressed uniquely in colonic epithelial cells (35).

Although both the enteroid and colonoid cultures were more similar to their tissues of origin, differences in mRNA transcript levels indicated that both organoid cultures retained an undifferentiated cell type phenotype with increased stem cells and decreased barrier maturation. Specifically, expression levels of genes encoding for markers of differentiated cell types such as *Atoh1*, *Cga*, and *Muc2* for

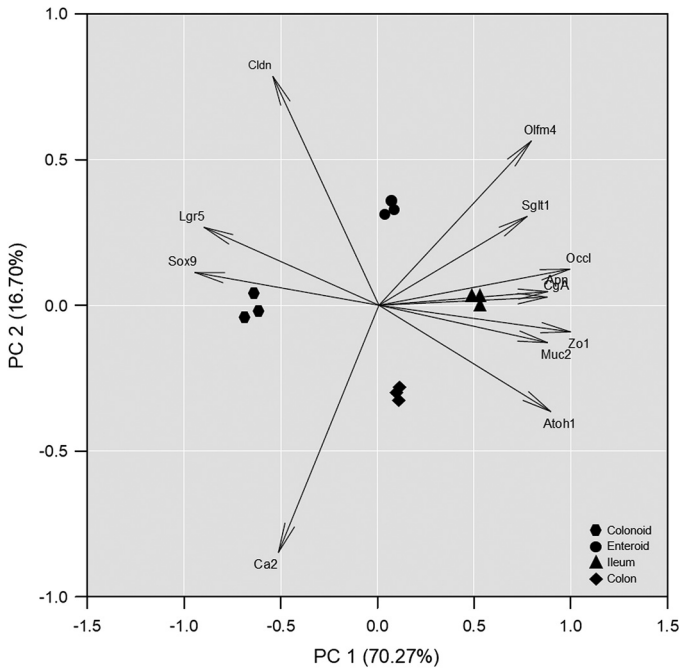

Figure 9. Principal component analysis (PCA) of gene expression data. Biplot resulting from a PCA of four samples (colonoids, enteroids, ileum, and colon) from three individual animals and 12 genes. The two principal components (PC1 and PC2) contribute to approximately 87% (70.3% and 16.7%) of the total variability. *Apn*, aminopeptidase N; *Atoh*, atonal homolog 1; *Ca2*, carbonic anhydrase 2; *Cga*, chromogranin A; *Cldn*, claudin; *Lgr5*, leucine-rich repeat-containing G protein-coupled receptor; *Muc2*, mucin 2; *Olfm4*, olfactomedin 4; *Sox9*, sex-determining region Y-box 9; *Sglt1*, sodium-glucose transporter 1; *Zo1*, zonula occludens 1.

secretory cell lineages in colonoid cultures and *Sglt1* and *Apn* for absorptive enterocytes in enteroid cultures were decreased, and in both organoid cultures, the levels of the stem cell markers *Lgr5* and *Sox9* were increased. In contrast, levels of *Occl* and *Zo1* were decreased. The undifferentiated, immature nature of both organoid cultures relative to their tissues observed in this study can be explained in part by the use of a conditioned medium that contained the essential factors Wnt, noggin, and R-spondin. The presence of Wnt ligands and R-spondin in the growth medium maintains the stem cell state through the activation of canonical Wnt signaling and the enhancement of Wnt/β-catenin signaling (36). Both *Lgr5* and *Sox9* are *Wnt* responsive gene targets (4, 37) and have crucial functions in stem cell maintenance as critical regulators of tissue homeostasis and regeneration in the intestine (38). Other signaling pathways such as BMP (noggin) and Egf also interact with the canonical Wnt pathway (36), regulate the number of stem cells through the suppression of Wnt signaling, and control the proliferation or the division rates of intestinal stem cells (39). For cultures such as colonoids and enteroids, maintaining the stem cell niche is imperative to ensure longevity over multiple passages, because without active stem cell populations, the regenerative capacity of such cultures would be lost (14).

Just as Wnt signaling regulates the stem cell state, other signaling pathways such as Notch signaling (40) control barrier maturation and cell fate decisions in the intestine and are implicated in the regulation of appropriate cell differentiation and cell regeneration (41). *Atoh1* is negatively regulated by active Notch signaling (2) and drives cell fate toward secretory cell lineages such as goblet and enteroendocrine cell types (42, 43). Consequently, a decrease in *Atoh1* expression, as observed for the colonoid cultures in this study, would result in decreased expression of secretory cell lineage markers. This decrease may have resulted from the inclusion of inhibitors to p38 mitogen-activated protein kinase (p38 MAPK) activity and TGFβ activity in addition to nicotinamide in the culture medium. It has been reported that inhibition of p38 activity decreases degradation of the epidermal growth factor receptor (EGFR) resulting in increased proliferation, decreased differentiation, and long-term maintenance of intestinal stem cells (36, 44).

In addition, p38 inhibitor treatment in vivo impeded goblet cell differentiation (45) and the inclusion of the p38 inhibitor and nicotinamide in the culture medium of human small intestinal enteroids strongly inhibited goblet and enteroendocrine cell differentiation relative to an ileal crypt fraction (3). The inclusion of the TGFβ inhibitor in the culture medium of colonoids and enteroids may have resulted in decreased *Ocln* expression through dysregulation of TGFβ receptor localization, which is required for efficient dissolution of tight junctions (46). An increase in *Cldn* mRNA expression was observed in both the enteroid and the colonoid cultures relative to their tissues of origin. This result contrasts with that of Pearce et al. (47), who reported *Cldn* expression levels in mouse enteroids were similar to that of isolated crypts or mucosal homogenates from the small intestine. The same study also reported that *Cldn* expression levels could change as a consequence of the cellular composition of the enteroid cultures (47). For example, murine enteroids with higher stem cell number (48) had increased *Cldn-2* and *Ocln* expression levels relative to enteroids with increased numbers of differentiated cell types such as enterocytes, enteroendocrine, or goblet cells. In contrast, *Zo1* expression was similar among all enteroid types regardless of the cellular composition (47). Consequently, regulation of TJ expression can vary among enteroids with different cellular compositions.

Conclusions

This study shows that long-term cultures of porcine colonoids can be isolated and maintained using published methods and media composition for porcine enteroid cultures with minor modifications. The mRNA expression profile of colonoids was most similar to an epithelial fraction from the colon and remained unchanged over several passages, and enteroid cultures were most like the ileal tissue from which they were derived. The media composition used in this study, with the essential factors Wnt, noggin, and R-spondin and inhibitors to cellular differentiation, predisposes these cultures to be undifferentiated with an increase in the abundance of stem cells and a decrease in differentiated cell types, especially those of the secretory cell lineage. For long-term colonoid cultures, this is desired because only stem cells have regenerative capabilities, and the loss of such cells would compromise the overall longevity of colonoids. Understanding these cultures with their multiple cell types and specific niche compartments and how they compare to the tissue of origin provides us with knowledge on the usability of such models in representing the in vivo situation.

GRANTS

A. M. Barnett was supported by a Postdoctoral Fellowship from the Riddet Institute Centre of Research Excellence, through funding provided by the New Zealand Tertiary Education Commission, and the New Zealand Ministry of Business, Innovation and Employment Endeavour research program New Zealand Milks Mean More (MAUX1803). Research funding was also provided by the Riddet Institute Centre of Research Excellence.

DISCLOSURES

No conflicts of interest, financial or otherwise, are declared by the authors.

AUTHOR CONTRIBUTIONS

A.M.B., J.A.M., and N.C.R. conceived and designed research; A.M.B., J.A.M., C.H., and L.L.B. performed experiments; A.M.B. and J.A.M. analyzed data; A.M.B., J.A.M., W.C.M., and N.C.R. interpreted results of experiments; A.M.B. prepared figures; A.M.B. drafted manuscript; A.M.B., J.A.M., W.C.M., and N.C.R. edited and revised manuscript; A.M.B., J.A.M., C.H., L.L.B., W.C.M., and N.C.R. approved final version of manuscript.

REFERENCES

1. **Barker N**, **van de Wetering M**, **Clevers H.** The intestinal stem cell. *Genes Dev* 22: 1856–1864, 2008. doi:10.1101/gad.1674008.
2. **VanDussen KL**, **Carulli AJ**, **Keeley TM**, **Patel SR**, **Puthoff BJ**, **Magness ST**, **Tran IT**, **Maillard I**, **Siebel C**, **Kolterud A**, **Grosse AS**, **Gumucio DL**, **Ernst SA**, **Tsai YH**, **Dempsey PJ**, **Samuelson LC.** Notch signaling modulates proliferation and differentiation of

intestinal crypt base columnar stem cells. *Development* 139: 488–497, 2012. doi:10.1242/dev.070763.

3. **Sato T**, **Stange DE**, **Ferrante M**, **Vries RG**, **Van Es JH**, **Van den Brink S**, **Van Houdt WJ**, **Pronk A**, **Van Gorp J**, **Siersema PD**, **Clevers H.** Long-term expansion of epithelial organoids from human colon, adenoma, adenocarcinoma, and Barrett's epithelium. *Gastroenterology* 141: 1762–1772, 2011. doi:10.1053/j.gastro.2011.07.050.
4. **van der Flier LG**, **Haegebarth A**, **Stange DE**, **van de Wetering M**, **Clevers H.** OLFM4 is a robust marker for stem cells in human intestine and marks a subset of colorectal cancer cells. *Gastroenterology* 137: 15–17, 2009. doi:10.1053/j.gastro.2009.05.035.
5. **Barnett AM**, **Roy NC**, **McNabb WC**, **Cookson AL.** Effect of a semi-purified oligosaccharide-enriched fraction from caprine milk on barrier integrity and mucin production of co-culture models of the small and large intestinal epithelium. *Nutrients* 8: 267, 2016. doi:10.3390/nu8050267.
6. **Brittan M**, **Wright NA.** Gastrointestinal stem cells. *J Pathol* 197: 492–509, 2002. doi:10.1002/path.1155.
7. **Hilgendorf C**, **Spahn-Langguth H**, **Regardh CG**, **Lipka E**, **Amidon GL**, **Langguth P.** Caco-2 versus Caco-2/HT29-MTX co-cultured cell lines: permeabilities via diffusion, inside- and outside-directed carrier-mediated transport. *J Pharm Sci* 89: 63–75, 2000. doi:10.1002/(sici)1520-6017(200001)89:1%3C63::aid-jps7%3E3.0.co;2-6.
8. **Kim YS**, **Ho SB.** Intestinal goblet cells and mucins in health and disease: recent insights and progress. *Curr Gastroenterol Rep* 12: 319–330, 2010. doi:10.1007/s11894-010-0131-2.
9. **Mahida YR.** Microbial-gut interactions in health and disease. Epithelial cell responses. *Best Pract Res Clin Gastroenterol* 18: 241–253, 2004. doi:10.1016/j.bpg.2003.10.001.
10. **Ulluwishewa D**, **Anderson RC**, **McNabb WC**, **Moughan PJ**, **Wells JM**, **Roy NC.** Regulation of tight junction permeability by intestinal bacteria and dietary components. *J Nutr* 141: 769–776, 2011. doi:10.3945/jn.110.135657.
11. **Ulluwishewa D**, **Anderson RC**, **Young W**, **McNabb WC**, **van Baarlen P**, **Moughan PJ**, **Wells JM**, **Roy NC.** Live *Faecalibacterium prausnitzii* in an apical anaerobic model of the intestinal epithelial barrier. *Cell Microbiol* 17: 226–240, 2015. doi:10.1111/cmi.12360.
12. **Gonzalez LM**, **Williamson I**, **Piedrahita JA**, **Blikslager AT**, **Magness ST.** Cell lineage identification and stem cell culture in a porcine model for the study of intestinal epithelial regeneration. *PLoS One* 8: e66465, 2013. doi:10.1371/journal.pone.0066465.
13. **Khalil HA**, **Lei NY**, **Brinkley G**, **Scott A**, **Wang J**, **Kar UK**, **Jabaji ZB**, **Lewis M**, **Martin MG**, **Dunn JC**, **Stelzner MG.** A novel culture system for adult porcine intestinal crypts. *Cell Tissue Res* 365: 123–134, 2016. doi:10.1007/s00441-016-2367-0.
14. **Sato T**, **Vries RG**, **Snippert HJ**, **van de Wetering M**, **Barker N**, **Stange DE**, **van Es JH**, **Abo A**, **Kujala P**, **Peters PJ**, **Clevers H.** Single Lgr5 stem cells build crypt-villus structures in vitro without a mesenchymal niche. *Nature* 459: 262–265, 2009. doi:10.1038/nature07935.
15. **van der Hee B**, **Loonen LMP**, **Taverne N**, **Taverne-Thiele JJ**, **Smidt H**, **Wells JM.** Optimized procedures for generating an enhanced, near physiological 2D culture system from porcine intestinal organoids. *Stem Cell Res* 28: 165–171, 2018. doi:10.1016/j.scr.2018.02.013.
16. **Kriz V**, **Korinek V.** Wnt, RSPO and Hippo signalling in the intestine and intestinal stem cells. *Genes (Basel)* 9: 20, 2018. doi:10.3390/genes9010020.
17. **Koltes DA**, **Gabler NK.** Characterization of porcine intestinal enteroid cultures under a lipopolysaccharide challenge1. *J Anim Sci* 94: 335–339, 2016. doi:10.2527/jas.2015-9793.
18. **Derricott H**, **Luu L**, **Fong WY**, **Hartley CS**, **Johnston LJ**, **Armstrong SD**, **Randle N**, **Duckworth CA**, **Campbell BJ**, **Wastling JM**, **Coombes JL.** Developing a 3D intestinal epithelium model for livestock species. *Cell Tissue Res* 375: 409–424, 2019. doi:10.1007/s00441-018-2924-9.
19. **Li L**, **Fu F**, **Guo S**, **Wang H**, **He X**, **Xue M**, **Yin L**, **Feng L**, **Liu P.** Porcine intestinal enteroids: a new model for studying enteric coronavirus porcine epidemic diarrhea virus infection and the host innate response. *J Virol* 93: e01682–01618, 2019. doi:10.1128/jvi.01682-18.
20. **Zhu M**, **Qin Y-C**, **Gao C-Q**, **Yan H-C**, **Wang X-Q.** l-Glutamate drives porcine intestinal epithelial renewal by increasing stem cell activity via upregulation of the EGFR-ERK-mTORC1 pathway. *Food Funct* 11: 2714–2724, 2020. doi:10.1039/C9FO03065D.
21. **Ripken D**, **Hendriks HFJ.** Porcine ex vivo intestinal segment model. In: *The Impact of Food Bioactives on Health: In Vitro and Ex Vivo Models*, edited by **Verhoeckx K**, **Cotter P**, **Lopez-Exposito I**, **Kleiveland C**, **Lea T**, **Mackie A**, **Requena T**, **Swiatecka D**, **Wichers H.** Cham: Springer International Publishing, 2015, p. 255–262. doi:10.1007/978-3-319-16104-4_23.
22. **Sciascia Q**, **Daş G**, **Metges CC.** REVIEW: The pig as a model for humans: effects of nutritional factors on intestinal function and health1. *J Anim Sci* 94: 441–452, 2016. doi:10.2527/jas2015-9788.
23. **Miyoshi H**, **Stappenbeck TS.** In vitro expansion and genetic modification of gastrointestinal stem cells in spheroid culture. *Nat Protoc* 8: 2471–2482, 2013. doi:10.1038/nprot.2013.153.
24. **Bartfeld S**, **Bayram T**, **van de Wetering M**, **Huch M**, **Begthel H**, **Kujala P**, **Vries R**, **Peters PJ**, **Clevers H.** In vitro expansion of human gastric epithelial stem cells and their responses to bacterial infection. *Gastroenterology* 148: 126–136.e126, 2015. doi:10.1053/j.gastro.2014.09.042.
25. **Cotton JL**, **Li Q**, **Ma L**, **Park JS**, **Wang J**, **Ou J**, **Zhu LJ**, **Ip YT**, **Johnson RL**, **Mao J.** YAP/TAZ and Hedgehog coordinate growth and patterning in gastrointestinal mesenchyme. *Dev Cell* 43: 35–47. e34, 2017. doi:10.1016/j.devcel.2017.08.019.
26. **Wu A**, **Yu B**, **Zhang K**, **Xu Z**, **Wu D**, **He J**, **Luo J**, **Luo Y**, **Yu J**, **Zheng P**, **Che L**, **Mao X**, **Huang Z**, **Wang L**, **Zhao J**, **Chen D.** Transmissible gastroenteritis virus targets Paneth cells to inhibit the self-renewal and differentiation of Lgr5 intestinal stem cells via Notch signaling. *Cell Death Dis* 11: 40, 2020. doi:10.1038/s41419-020-2233-6.
27. **Tegel H**, **Dannemeyer M**, **Kanje S**, **Sivertsson Å**, **Berling A**, **Svensson A-S**, **Hober A**, **Enstedt H**, **Volk A-L**, **Lundqvist M**, **Moradi M**, **Afshari D**, **Ekblad S**, **Xu LLan**, **Westin M**, **Bidad F**, **Schiavone LH**, **Davies R**, **Mayr LM**, **Knight S**, **Göpel SO**, **Voldborg BG**, **Edfors F**, **Forsström B**, **von Feilitzen K**, **Zwahlen M**, **Rockberg J**, **Takanen JO**, **Uhlén M**, **Hober S.** High throughput generation of a resource of the human secretome in mammalian cells. *N Biotechnol* 58: 45–54, 2020. doi:10.1016/j.nbt.2020.05.002.
28. **Nygard AB**, **Jorgensen CB**, **Cirera S**, **Fredholm M.** Selection of reference genes for gene expression studies in pig tissues using SYBR green qPCR. *BMC Mol Biol* 8: 67, 2007. doi:10.1186/1471-2199-8-67.
29. **Willing BP**, **Van Kessel AG.** Intestinal microbiota differentially affect brush border enzyme activity and gene expression in the neonatal gnotobiotic pig. *J Anim Physiol Anim Nutr (Berl)* 93: 586–595, 2009. doi:10.1111/j.1439-0396.2008.00841.x.
30. **Tossou MC**, **Liu H**, **Bai M**, **Chen S**, **Cai Y**, **Duraipandiyan V**, **Liu H**, **Adebowale TO**, **Al-Dhabi NA**, **Long L**, **Tarique H**, **Oso AO**, **Liu G**, **Yin Y.** Effect of high dietary tryptophan on intestinal morphology and tight junction protein of weaned pig. *Biomed Res Int* 2016: 1–6, 2016. doi:10.1155/2016/2912418.
31. **Livak KJ**, **Schmittgen TD.** Analysis of relative gene expression data using real-time quantitative PCR and the $2^{-\Delta\Delta C}_T$ method. *Methods* 25: 402–408, 2001. doi:10.1006/meth.2001.1262.
32. **Rohart F**, **Gautier B**, **Singh A**, **Le CK.** mixOmics: an R package for 'omics feature selection and multiple data integration. *PLoS Comput Biol* 13: e1005752, 2017. doi:10.1371/journal.pcbi.1005752.
33. **Costa J**, **Ahluwalia A.** Advances and current challenges in intestinal *in vitro* model engineering: a digest. *Front Bioeng Biotechnol* 7: 144, 2019. doi:10.3389/fbioe.2019.00144.
34. **Kraiczy J**, **Nayak KM**, **Howell KJ**, **Ross A**, **Forbester J**, **Salvestrini C**, **Mustata R**, **Perkins S**, **Andersson-Rolf A**, **Leenen E**, **Liebert A**, **Vallier L**, **Rosenstiel PC**, **Stegle O**, **Dougan G**, **Heuschkel R**, **Koo BK**, **Zilbauer M.** DNA methylation defines regional identity of human intestinal epithelial organoids and undergoes dynamic changes during development. *Gut* 68: 49–61, 2019. doi:10.1136/gutjnl-2017-314817.
35. **Tetteh PW**, **Kretzschmar K**, **Begthel H**, **van den Born M**, **Korving J**, **Morsink F**, **Farin H**, **van Es JH**, **Offerhaus GJ**, **Clevers H.** Generation of an inducible colon-specific Cre enzyme mouse line for colon cancer research. *Proc Natl Acad Sci USA* 113: 11859–11864, 2016. doi:10.1073/pnas.1614057113.
36. **Holmberg FE**, **Seidelin JB**, **Yin X**, **Mead BE**, **Tong Z**, **Li Y**, **Karp JM**, **Nielsen OH.** Culturing human intestinal stem cells for regenerative applications in the treatment of inflammatory bowel disease. *EMBO Mol Med* 9: 558–570, 2017. doi:10.15252/emmm.201607260.
37. **Smith NR**, **Gallagher AC**, **Wong MH.** Defining a stem cell hierarchy in the intestine: markers, caveats and controversies. *J Physiol* 594: 4781–4790, 2016. doi:10.1113/JP271651.

38. **Carrasco-Garcia E**, **Lopez L**, **Aldaz P**, **Arevalo S**, **Aldaregia J**, **Egana L**, **Bujanda L**, **Cheung M**, **Sampron N**, **Garcia I**, **Matheu A.** SOX9-regulated cell plasticity in colorectal metastasis is attenuated by rapamycin. *Sci Rep* 6: 32350, 2016. doi:10.1038/srep32350.
39. **Gehart H**, **Clevers H.** Tales from the crypt: new insights into intestinal stem cells. *Nat Rev Gastroenterol Hepatol* 16: 19–34, 2019. doi:10.1038/s41575-018-0081-y.
40. **Nakamura T**, **Nakamura T**, **Matsumoto K.** The functions and possible significance of Kremen as the gatekeeper of Wnt signalling in development and pathology. *J Cell Mol Med* 12: 391–408, 2008. doi:10.1111/j.1582-4934.2007.00201.x.
41. **Santos AJM**, **Lo YH**, **Mah AT**, **Kuo CJ.** The intestinal stem cell niche: homeostasis and adaptations. *Trends Cell Biol* 28: 1062–1078, 2018. doi:10.1016/j.tcb.2018.08.001.
42. **Okamoto R**, **Tsuchiya K**, **Nemoto Y**, **Akiyama J**, **Nakamura T**, **Kanai T**, **Watanabe M.** Requirement of Notch activation during regeneration of the intestinal epithelia. *Am J Physiol Gastrointest Liver Physiol* 296: G23–G35, 2009. doi:10.1152/ajpgi.90225.2008.
43. **Van Landeghem L**, **Santoro MA**, **Krebs AE**, **Mah AT**, **Dehmer JJ**, **Gracz AD**, **Scull BP**, **McNaughton K**, **Magness ST**, **Lund PK.** Activation of two distinct Sox9-EGFP-expressing intestinal stem cell populations during crypt regeneration after irradiation. *Am J Physiol Gastrointest Liver Physiol* 302: G1111–G1132, 2012. doi:10.1152/ajpgi.00519.2011.
44. **Frey MR**, **Golovin A**, **Polk DB.** Epidermal growth factor-stimulated intestinal epithelial cell migration requires Src family kinase-dependent p38 MAPK signaling. *J Biol Chem* 279: 44513–44521, 2004. doi:10.1074/jbc.M406253200.
45. **Otsuka M**, **Kang YJ**, **Ren J**, **Jiang H**, **Wang Y**, **Omata M**, **Han J.** Distinct effects of p38alpha deletion in myeloid lineage and gut epithelia in mouse models of inflammatory bowel disease. *Gastroenterology* 138: 1255–1265, 2010. doi:10.1053/j.gastro.2010.01.005.
46. **Barrios-Rodiles M**, **Brown KR**, **Ozdamar B**, **Bose R**, **Liu Z**, **Donovan RS**, **Shinjo F**, **Liu Y**, **Dembowy J**, **Taylor IW**, **Luga V**, **Przulj N**, **Robinson M**, **Suzuki H**, **Hayashizaki Y**, **Jurisica I**, **Wrana JL.** High-throughput mapping of a dynamic signaling network in mammalian cells. *Science* 307: 1621–1625, 2005. doi:10.1126/science.1105776.
47. **Pearce SC**, **Al-Jawadi A**, **Kishida K**, **Yu S**, **Hu M**, **Fritzky LF**, **Edelblum KL**, **Gao N**, **Ferraris RP.** Marked differences in tight junction composition and macromolecular permeability among different intestinal cell types. *BMC Biol* 16: 19, 2018. doi:10.1186/s12915-018-0481-z.
48. **Kishida K**, **Pearce SC**, **Yu S**, **Gao N**, **Ferraris RP.** Nutrient sensing by absorptive and secretory progenies of small intestinal stem cells. *Am J Physiol Gastrointest Liver Physiol* 312: G592–G605, 2017. doi:10.1152/ajpgi.00416.2016.